THE ASTROPHYSICAL JOURNAL, 304:241–248, 1986 May 1

ORBITAL ELEMENTS OF THE BINARY X-RAY PULSAR GX 301-2

N. SATO AND F. NAGASE
Department of Astrophysics, Nagoya University, Japan
N. KAWAI
Institute of Space and Astronautical Science, Japan
R. L. KELLEY[1]
Laboratory for High Energy Astrophysics, NASA/Goddard Space Flight Center
S. RAPPAPORT
Department of Physics and Center for Space Research, Massachusetts Institute of Technology
AND
N. E. WHITE
Space Science Department of the European Space Agency, European Space Research and Technology Center, Noordwijk, The Netherlands
Received 1985 April 8; accepted 1985 October 23

ABSTRACT

X-ray outbursts from GX 301-2 were observed with *Hakucho* on two occasions during 1982 April and May and with *Tenma* in 1984 April. Pulse arrival times measured with *Hakucho* were combined with those previously measured with *Ariel 5* and *SAS 3*. The joint timing analysis of these data sets yields an orbital period of 41.5 days as the only acceptable solution; this is consistent with the period derived from the X-ray flaring events of the source. The orbital elements of the binary system, established from the joint timing analysis, are presented. Our orbital solution suggests that all the peaks of X-ray flares observed during the past 10 yr occur at the orbital period, but consistently appear ~ 1.4 days before the time of periastron passage of the X-ray star.

Subject headings: stars: individual — X-rays: binaries

I. INTRODUCTION

The X-ray source GX 301-2/4U 1223-62 was discovered as a moderately intense source with a hard energy spectrum (Ricker *et al.* 1973). Its optical counterpart was identified with an early-type supergiant (B1.5 Ia), Wray 977 (Vidal 1973; Bradt *et al.* 1977). X-ray pulsations from GX 301-2 with a period of 11.6 minutes (~ 700 s) were discovered by White *et al.* (1976).

Many attempts have been made to determine the orbital period of this binary system. White, Mason, and Sanford (1978, hereafter WMS) obtained an orbital period of 40.8 days from a pulse-timing analysis based on *Ariel 5* observations. Kelley, Rappaport, and Petre (1980, hereafter KRP) also performed a pulse-timing analysis by combining *SAS 3* data with the WMS *Ariel 5* data. They obtained several acceptable solutions for the orbital period which could be expressed as $P_{\rm orb} \approx 456/n$ days, where n is an integer $\lesssim 20$. Orbital solutions with periods of 35.0 and 32.5 days were suggested as the most compatible with all the available data. Various optical studies have also been made using spectroscopic and photometric observations of the optical counterpart Wray 977 (Bord *et al.* 1976; Hammerschlag-Hensberge *et al.* 1976; Mauder and Ammann 1976; van Genderen 1977; Pakull 1978). However, the orbital periods suggested from the optical data are neither consistent with each other nor in agreement with the X-ray periods.

More recently, Watson, Warwick, and Corbet (1982, hereafter WWC) have reported a period of 41.5 days on the basis of the periodicity in X-ray flaring events of GX 301-2 observed with *Ariel 5*. This value is close to another candidate orbital period, 41.4 days, in the solutions derived from the pulse-timing analysis of KRP. Priedhorsky and Terrell (1983) have also confirmed the 41.5 day periodicity by a time series analysis of the X-ray intensity of GX 301-2 based on *Vela* satellite observations between 1969 and 1976. They give 41.52 ± 0.02 days as the best estimate of the flare recurrence period based on both the *Ariel 5* and the *Vela* satellite X-ray photometric data. Reexamining the *Ariel 5*/*SAS 3* joint pulse timing analysis, White and Swank (1984, hereafter WS) have obtained an orbital period of 41.46 ± 0.04 days.

The X-ray pulsar GX 301-2 was observed with the *Hakucho* satellite during the period 1982 April 6–20 and May 16–21. The details of these observations have been described by Mitani *et al.* (1984), in which they also discuss the time variability of the X-ray intensity and the pulse profile. Kawai *et al.* (1985) carried out a timing analysis of these data in which, because of the relatively short duration of the *Hakucho* data, they allowed $P_{\rm orb}$ to be a free parameter but held the remaining orbital parameters fixed at the values given by WS. The long baseline between the *Ariel 5*/*SAS 3* observations and the *Hakucho* observation enabled them to determine the orbital period more accurately than WS, and they obtained 41.524 ± 0.006 days. Hence, an orbital period of 41.5 days is consistently supported both by the pulse timing and the X-ray photometric (i.e., flares) analyses.

In order to establish definitively the orbital elements of the GX 301-2/Wray 977 system, we have carried out a joint fit to the combined pulse arrival time data obtained with *Ariel 5*, *SAS 3*, and *Hakucho*. We obtain a unique set of orbital elements with an orbital period of 41.51 days. The details of the analysis and the full orbital solutions are described in § II. We find that the difference between the time of maximum X-ray intensity and periastron passage of the X-ray star is ~ 1.4 days.

[1] NAS/NRC Research Associate.

GX 301-2 was also observed recently with the *Tenma* satellite during the interval 1984 April 21–27. The light curve and the energy spectrum observed with *Tenma* are described by Makino, Leahy, and Kawai (1985). The pulse arrival times measured during this interval were used in the present analysis to further confirm the orbital parameters.

II. TIMING ANALYSIS OF JOINT DATA SETS

In the present joint analysis, we have used the following four data sets: (1) 114 pulse arrival times measured with *Ariel 5* over an interval of 61 days from 1977 September 7 to November 6, (2) 109 arrival times measured with *SAS 3* during the interval 1979 January 20 to February 19, (3) 39 arrival times measured with *Hakucho* during 1982 April 6–20, and (4) 27 arrival times measured with *Hakucho* during 1982 May 16–21. Detailed descriptions of the individual data sets are presented by WMS for data set (1), KRP for (2), and Kawai *et al.* (1985) for (3) and (4).

An additional data set consisting of 13 pulse arrival times is also available from observations made with *Tenma* during the 3 day interval 1984 April 24–27. However, this data set is not included in the first step of the analysis since the observation interval is too short to play an effective role in the determination of the orbit.

In our analysis of the *Ariel 5*, *SAS 3*, and *Hakucho* data we found that the pulse arrival times could be tracked coherently throughout each of the observation intervals, but not over the gap between the data sets. Accordingly, the pulse arrival time t_{nk} of the nth pulse in the kth data set was fitted to the function

$$t_{nk} = T_k + P_k n + \tfrac{1}{2}P_k \dot{P}_k n^2 + \tfrac{1}{6}P_k^2 \ddot{P}_k n^3 + a_x \sin i \, F(e, \omega, \tau, \theta) , \quad (1)$$

where P_k is the pulse period at the initial epoch T_k in the kth data set. The quantities $\dot{P}_k$ and $\ddot{P}_k$ are the first and second time derivatives of the pulse period respectively. The last term in equation (1) represents the Doppler delays caused by an eccentric orbit with projected semimajor axis $a_x \sin i$, eccentricity e, longitude of periastron ω, time of periastron passage τ, and mean anomaly θ. The mean anomaly is given by $\theta = 2\pi(t - \tau)/P_{\rm orb}$, where $P_{\rm orb}$ is the orbital period. All the orbital elements, $a_x \sin i$, e, ω, τ, and $P_{\rm orb}$ were assumed to be constant during the interval between 1977 and 1982. The subscript k for T, P, $\dot{P}$, and $\ddot{P}$ runs from 1 to 4, corresponding to data sets (1)–(4).

In the fitting procedure, we included terms representing changes in the intrinsic pulse period in the following manner: (*a*) both $\dot{P}$ and $\ddot{P}$ are free parameters for $k = 1$; (*b*) only $\dot{P}$ is a free parameter for $k = 2$ and $k = 3$; and (*c*) $\dot{P} = \ddot{P} = 0$ for $k = 4$. The validity of this choice of $\dot{P}$- and $\ddot{P}$-terms will be discussed later. In the following fits, we also adopted the errors in pulse arrival times determined by WMS for *Ariel 5* data, by KRP for *SAS 3* data, and by Kawai *et al.* (1985) for the *Hakucho* data, although their methods of error determination are each somewhat different.

As a first step, we held the orbital period $P_{\rm orb}$ fixed at various trial values between 15 and 70 days and fitted for the remaining 16 parameters. The orbital period was incremented in 1 day steps, thus yielding a minimum χ^2 versus orbital period. Next, detailed fits were made in the vicinity of each local χ^2 minimum that was obtained. In this case all 17 parameters, including the orbital period, were taken to be free parameters.

The reduced χ^2 values (χ^2_ν) obtained by this procedure are plotted against orbital period in Figure 1. The smallest value of χ^2_ν (1.16) is obtained for an orbital period of 41.5 days. One can clearly see several local minima around 32.5, 35, 38, 45, and 57 days (these values correspond to the solutions derived by KRP as seen in their Table 1). However, these alternate periods can now be rejected, because the corresponding χ^2 values are twice as large as that for an orbital period of 41.5 days. The acceptable values of χ^2_ν are formally 1.11 and 1.20 for confidence limits of 90% and 99% respectively, for the case of 273 degrees of freedom. Hence, the orbital period of 41.51 days is the only formally acceptable solution.

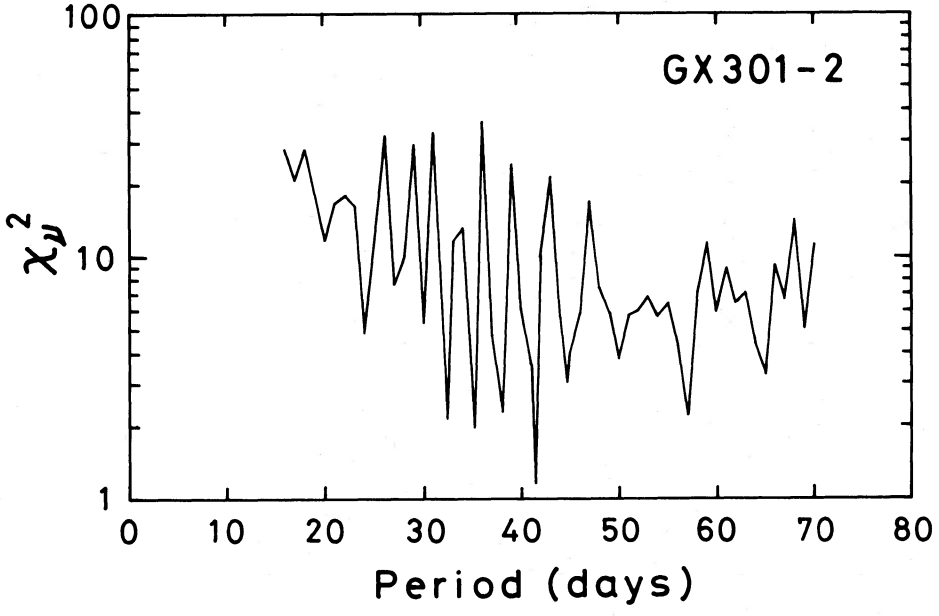

FIG. 1.—Reduced χ^2 vs. trial orbital period for GX 301-2 based on *Ariel 5*, *SAS 3*, and *Hakucho* timing data. The reduced χ^2 values were obtained by holding the orbital period fixed at each trial value and optimizing the remaining parameters (see text) and are shown for periods in the range 15–70 days.

From our fits to all the orbital parameters (in the vicinity of $P_{orb} = 41.5$ days), we obtained a best-fit orbital period of 41.508 ± 0.007 days (all errors cited are single-parameter 1 σ confidence limits). The best-fit values of the parameters are listed in Table 1. The Doppler delays estimated from the best-fit parameters in Table 1 are compared with the *Ariel 5*, *SAS 3*, and *Hakucho* pulse arrival times in Figure 2.

One might suspect that the choice of the $\dot{P}$ and $\ddot{P}$ terms would affect the resulting values of the best-fit parameters. To examine this question, we performed fits with several combinations of $\dot{P}$ and $\ddot{P}$ for the various data sets and found that the inclusion of such higher order terms did not substantially improve the fits. In most cases, the best-fit orbital parameters derived with the higher order terms were consistent with those in Table 1, within the accuracy of the determinations. This result can be understood in term of the relatively short duration of the *Hakucho* data sets.

Finally, we used equation (1) to fit jointly the pulse arrival times of the four data sets discussed above in addition to a fifth data set obtained with *Tenma* ($k = 5$). For this fifth data set we assumed that $\dot{P}_5 = \ddot{P}_5 = 0$ (the time span of these data is only 3 days). We find that fits starting with values of P_{orb} around 41.5 days yield best-fit parameters and pulse periods which are consistent with those derived from the joint fits without the *Tenma* data set. All parameters derived from the fits with and without *Tenma* data are completely self-consistent. A pulse period of 701.14 ± 0.03 s was determined for the *Tenma* data set of 1984 April. This value is the largest of the periods thus far observed for GX 301-2.

TABLE 1

ORBITAL ELEMENTS OF THE GX 301-2 SYSTEM AND PULSE PERIOD PARAMETERS[a]

Parameter	Value
Orbital Elements	
P_{orb} (days)	41.508 ± 0.007
$a_x \sin i$ (lt-sec)	371.2 ± 3.3
$f(M)$ ($M_\odot$)	31.9 ± 0.8
e	0.472 ± 0.011
ω	$-50\overset{\circ}{.}1 \pm 2\overset{\circ}{.}6$
τ (JD)	$2{,}443{,}906.56 \pm 0.16$
Pulse Periods	
Ariel 5:	
P_1 (s)	696.665 ± 0.017
$\dot{P}_1$	$-2.44 \pm 0.19 \times 10^{-7}$
$\ddot{P}_1$ (s^{-1})	$7.4 \pm 0.8 \times 10^{-14}$
SAS 3:	
P_2 (s)	698.376 ± 0.015
$\dot{P}_2$	$-0.68 \pm 0.10 \times 10^{-7}$
Hakucho:	
P_3 (s)	697.538 ± 0.041
$\dot{P}_3$	$4.66 \pm 0.64 \times 10^{-7}$
P_4 (s)	698.246 ± 0.043

[a] All quoted uncertainties are single-parameter 1 σ confidence limits.

III. DISCUSSION

We have found from a joint timing analysis of *Ariel 5*, *SAS 3*, and *Hakucho* data sets of pulse arrival times from GX 301-2 that an orbital period of 41.508 days is the uniquely acceptable solution. This value for the orbital period is consistent with that derived by WWC and by Priedhorsky and Terrell (1983) to within the accuracy of those determinations. The present analysis has improved the accuracy of the orbital period and has established definitive orbital parameters for the GX 301-2/Wray 977 binary system. A schematic orbit corresponding to

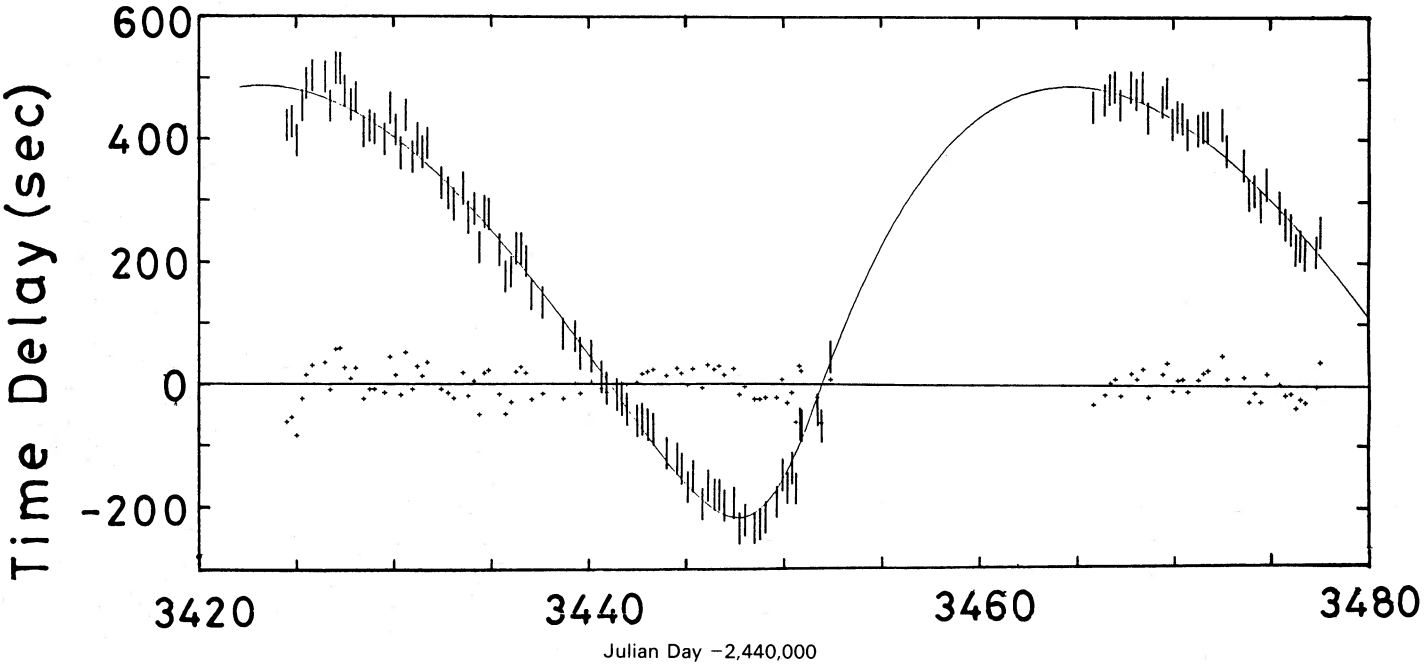

FIG. 2a

FIG. 2.—Doppler delay curves for GX 301-2, from (*a*) *Ariel 5*, (*b*) *SAS 3*, and (*c*) *Hakucho*. Solid curves represent the delays predicted from the orbital parameters in Table 1. The vertical bars are the measured delays after subtracting the delays due to a constant pulse period and changes in the intrinsic period. The dots are the residual differences between the measured delays and the fitted orbit.

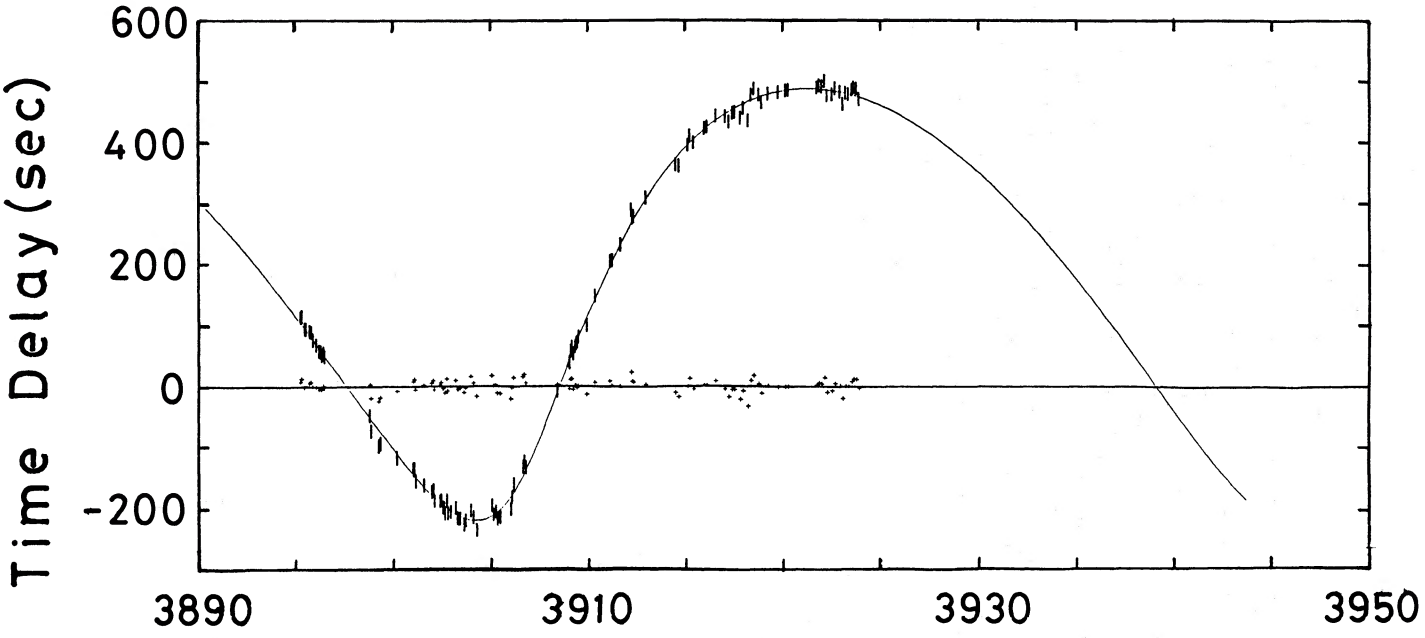

FIG. 2*b*

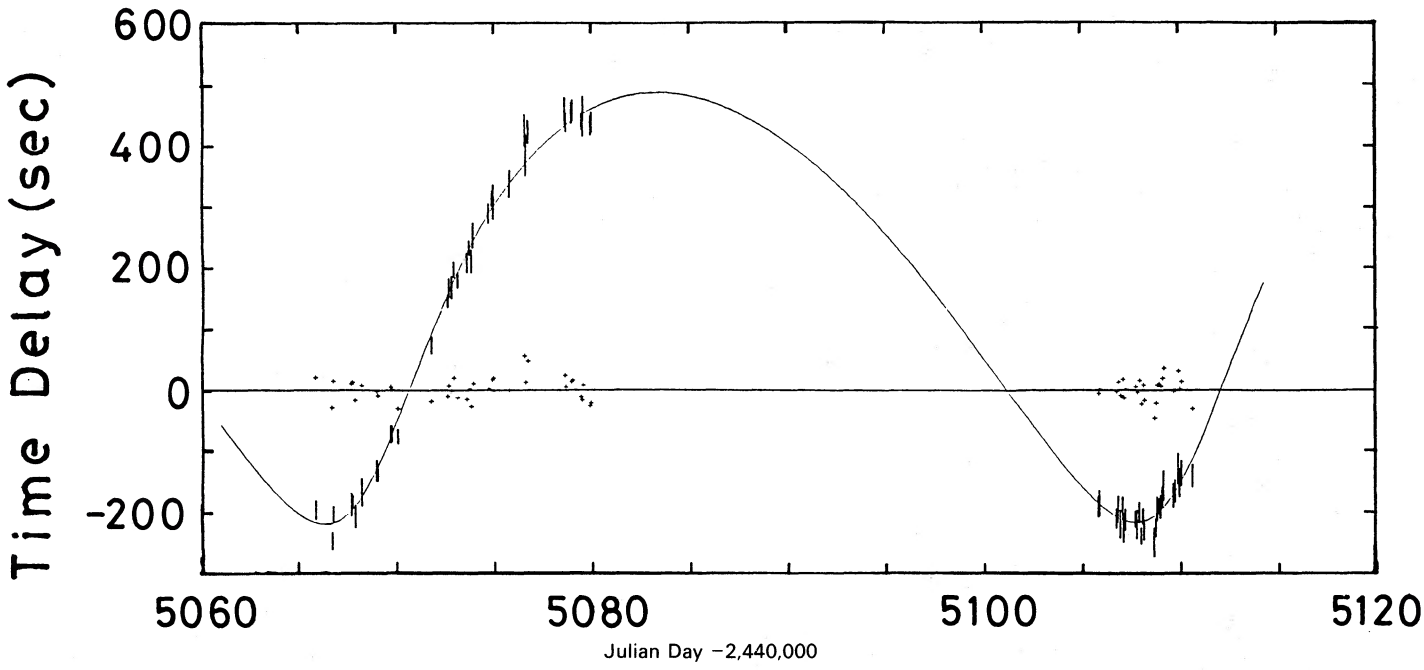

FIG. 2*c*

the best-fit parameters is shown in Figure 3 for an inclination angle $i = 90°$ and an assumed mass $M_{opt} = 30\ M_\odot$ and radius $R_{opt} = 43\ R_\odot$ (Parkes *et al.* 1980) for the companion star Wray 977. This binary system, GX 301-2/Wray 977, has the most eccentric orbit ($e = 0.47$) and the largest mass function [$f(M) = 32\ M_\odot$] among the ~ 10 binary X-ray pulsars for which the orbital parameters have been determined (see, e.g., Joss and Rappaport 1984).

The mass of the optical counterpart has been estimated to be $M_{opt} = 30 \pm 5\ M_\odot$ by Parkes *et al.* (1980) from their spectroscopic observations of Wray 977. Our determination of the mass function, $f(M) = 31.9 \pm 0.8\ M_\odot$, yields a lower limit to $f(M)$ of 30.3 $M_\odot$ (2 σ confidence limit), which, in turn, yields the constraint $M_{opt} \gtrsim 33\ M_\odot$, for an assumed mass of 1.4 $M_\odot$ for the neutron star (Joss and Rappaport 1984). From the lack of X-ray eclipses, which would occur around orbital phase $\phi \approx 0.2$ (see Fig. 3), the limit on inclination angle is estimated to be $i \lesssim 78°$. This increases the lower limit on the primary mass to $M_{opt} \gtrsim 35\ M_\odot$. A plausible set of parameters is $i \approx 75°$ and $M_{opt} \approx 38\ M_\odot$, which takes into account all the X-ray and optical constraints.

Because of the correlation between orbital elements and

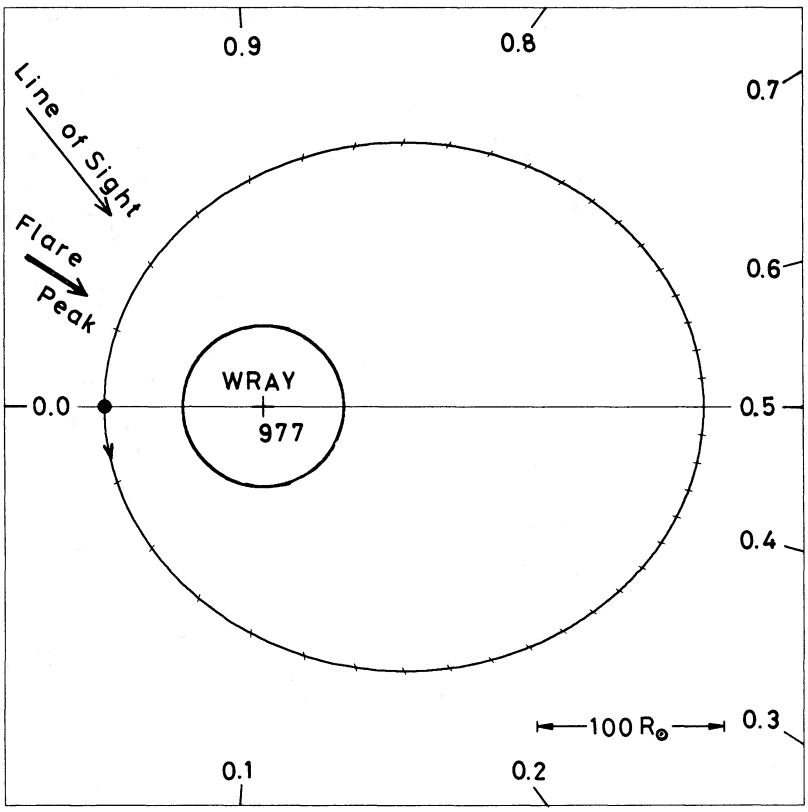

FIG. 3.—Schematic view of the GX 301-2/Wray 977 binary system, based on the orbital parameters in Table 1 with assumed values of $R_{opt} = 43\ R_\odot$ and $i = 90°$. Orbital phases are marked around the perimeter of the figure. The phase of the X-ray flare peak is indicated by the double arrow.

pulse periods that can occur when complete orbital phase coverage is unavailable, a poor determination of orbital parameters will often yield systematic errors in the determination of pulse periods and their intrinsic changes. Since we have now established the binary orbit, we were able to revise the pulse periods and their rates of intrinsic change for the data sets used in the analysis as well as from other previous observations. The revised pulse period values (see Table 1) are shown in Figure 4 along with the history of long-term changes in pulse period. Those values which are plotted as circled dots with attached arrows indicate the changes in intrinsic period directly measured during the observations. It is clear that GX 301-2 exhibits both spin-up and spin-down episodes on time scales of weeks to years. This behavior is quite similar to that of Vela X-1 (Nagase *et al.* 1984) and may be associated with the fact that both these systems are stellar wind–driven X-ray sources. As the orbit of the GX 301-2 system becomes even more precisely determined, detailed studies of pulse period change, such as the timing–noise power analysis made by Boynton *et al.* (1984) for Vela X-1, may become a promising technique for investigating the behavior of the stellar wind and the structure of the neutron star in the GX 301-2 system.

WWC suggested that there was a 1–5 day difference between the time of flare maximum and the time of periastron passage, based on the flare data and obital solution then available. In Figure 5, we show the X-ray light curves near the time of periastron passage as observed by *Ariel 5* (WWC), *SAS 3* (KRP), and *Hakucho* (Mitani *et al.* 1984), where phase zero refers to the time of periastron passage as determined from the present analysis (Table 1). We determine that the flare maximum slightly precedes periastron passage by ~ 1 day. To study the difference between the times of flare peak and periastron passage, we fitted all the published epochs of flare maximum (Priedhorsky and Terrell 1983; WWC; KRP; Mitani *et al.* 1984; Rothschild and Soong 1983, 1985) to the linear function $T_{FN} = T_{F0} + P_F N$, with an epoch, T_{F0}, and flare period, P_F, as free parameters. The epoch of flare center measured with *Tenma* in 1984 April is also included in the fit. From the fit to the above data, we determined the following X-ray flare ephemeris:

$$T_{F0} = \text{JD } 2{,}443{,}905.27 \pm 0.49\ ,$$
$$P_F = 41.519 \pm 0.012 \text{ days}\ , \qquad (2a)$$

with a minimum χ^2_ν of 0.14. The residuals from the best-fit ephemeris are shown in Figure 6. The unreasonably small value of χ^2_ν is most likely caused by conservatively overestimated errors in the published flare epochs. By rescaling all the errors with a multiplicative factor of 0.374 (as indicated by the thick error bars in Fig. 6) to give a $\chi^2_\nu = 1$, we obtain the following ephemeris:

$$T_{F0} = \text{JD } 2{,}443{,}905.27 \pm 0.19\ ,$$
$$P_F = 41.519 \pm 0.005 \text{ days}\ . \qquad (2b)$$

Finally, as a test of how sensitive the best-fit parameters are to the assumed error bars, we carried out a fit where all the points are given equal weight and adjusted to give a $\chi^2_\nu = 1$:

$$T_{F0} = \text{JD } 2{,}443{,}905.35 \pm 0.21\ ,$$
$$P_F = 41.514 \pm 0.007 \text{ days}\ . \qquad (2c)$$

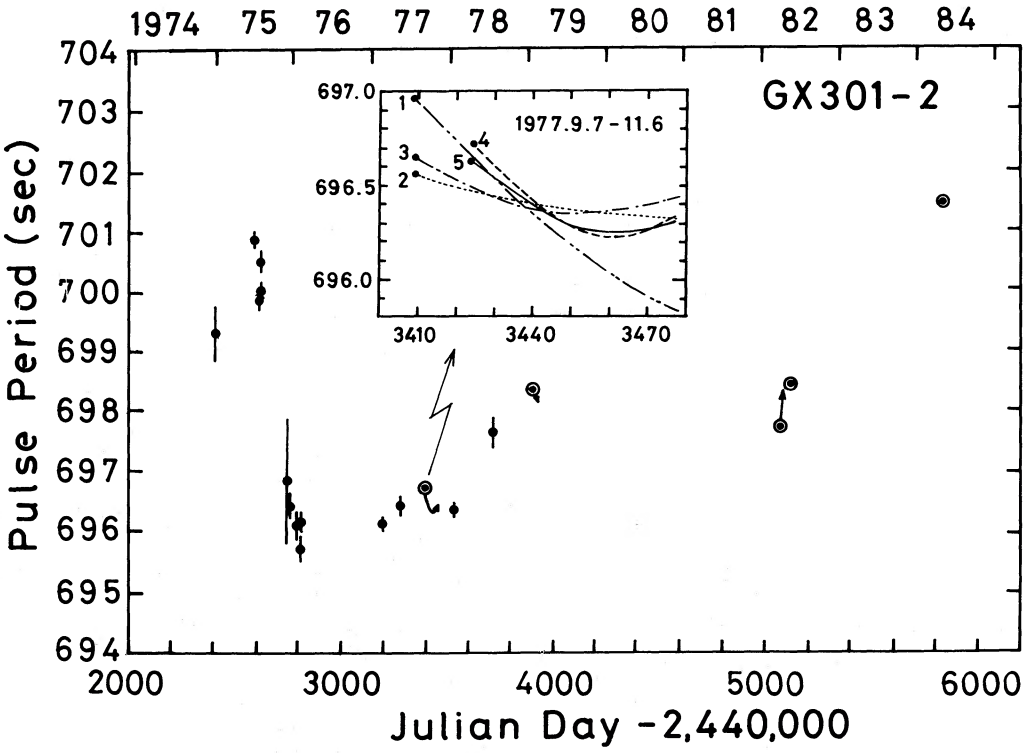

FIG. 4

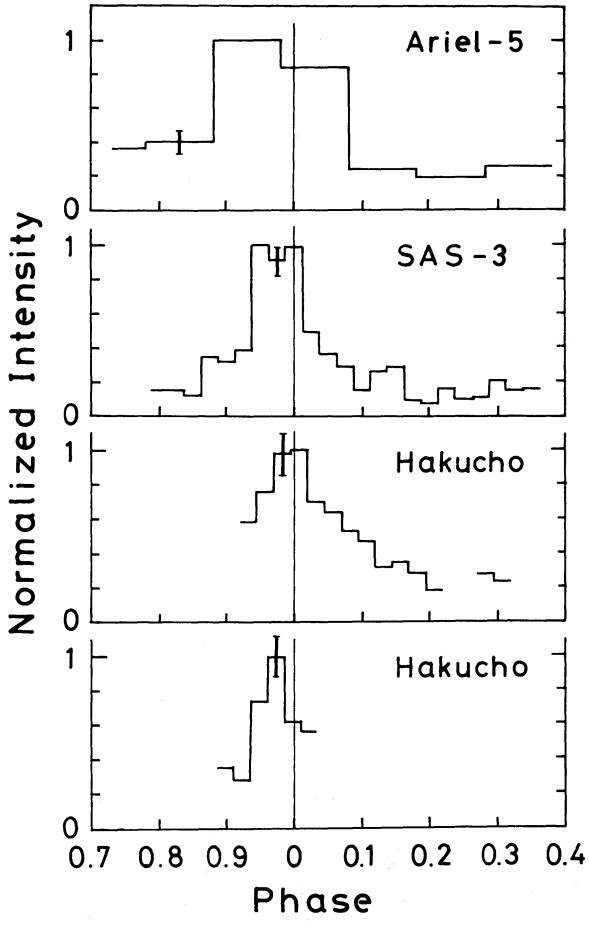

FIG. 5

FIG. 4.—Long-term pulse period history of GX 301-2. The circled points indicate pulse period measurements that have been revised slightly by the present orbital analysis. The arrows associated with the circled points indicate the short-term period changes during a given continuous observation. Previous results are adopted from KRP and from WS, whereas the point in 1984 is based on *Tenma* data. The insert is a magnified view of the changes in intrinsic period during the interval 1977 September–November. The curves in the insert are labeled by the different orbital solutions used to derive them: curves 1–5 are based on the orbital solutions of WMS (1), KRP (2 and 3), WS (4), and present work (5). These curves illustrate the importance of establishing the orbital parameters of a binary system before investigating the behavior of the intrinsic pulse period changes.

FIG. 5.—Flare profiles from GX 301-2 near times of periastron passage as observed with *Ariel 5* (WWC), *SAS 3* (KRP), and *Hakucho* (Mitani *et al.* 1984). Phase zero corresponds to the time of periastron passage (see Table 1).

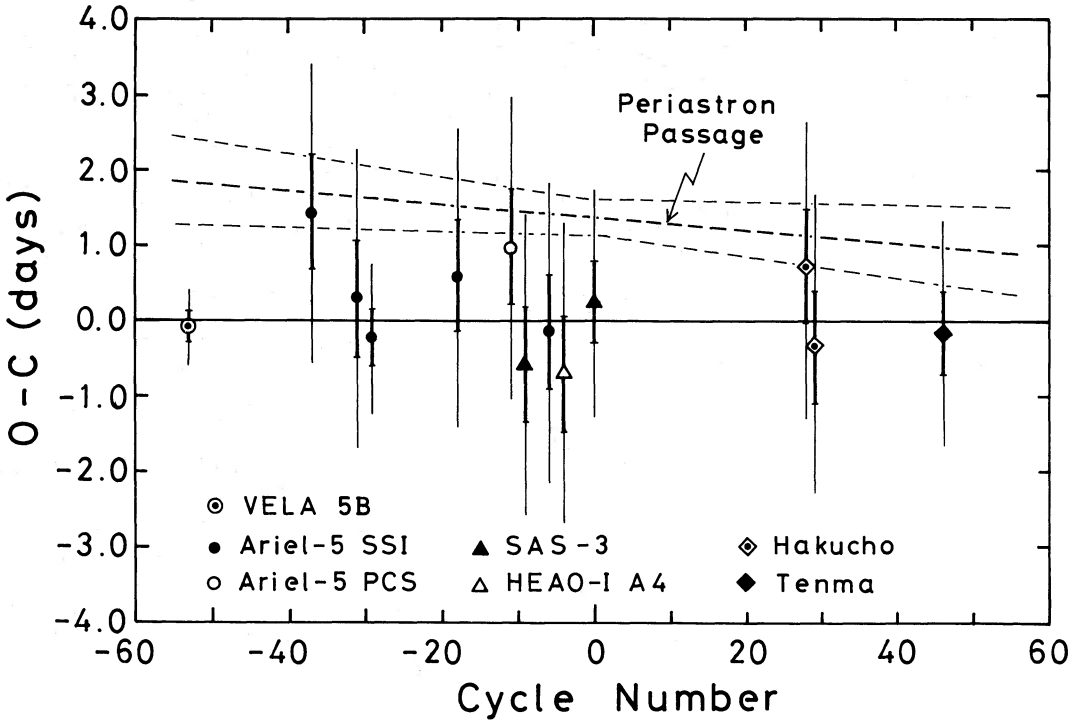

FIG. 6.—The residuals of the observed X-ray flare maxima with respect ot the ephemeris given in the text (see eq. [2a]). Data from Priedhorsky and Terrell (1983), WWC, KRP, Mitani *et al.* (1984), and Rothschild and Soong (1985). The data point at orbital cycle 46 is derived from *Tenma* data. Cycle zero is arbitrarily defined to coincide with the *SAS 3* observation in 1979. The thin and thick vertical bars correspond to the published and the renormalized (see text) uncertainties respectively. The dashed line represents the time of periastron passage predicted from the best-fit orbital parameters (Table 1). Note that the slope of the dashed line is essentially consistent with zero (i.e., $P_F - P_{orb} = 0.011 \pm 0.009$ days).

The values and the errors in equation (2c) are consistent with those given in equation (2b).

The result that the recurrence period of the X-ray flares is consistent with the orbital period ($P_F - P_{orb} = 0.011 \pm 0.009$ days; based on eq. [2b]) indicates that the outbursts of GX 301-2 are in fact caused by the orbital motion of the neutron star. Furthermore, the difference between the flare center and the time of periastron passage,

$$\Delta T_F = T_{F0} - \tau = -1.39 \pm 0.25 \text{ days},$$
$$\text{or } \Delta\Phi_F = -0.034 \pm 0.007, \quad (3)$$

is small but is significant at the 5 σ confidence level. All the flare peaks systematically occur ~ 1.4 days before periastron passage with a small jitter (~ 0.3 days), as can be seen in Figure 6. The time difference of 1.2 ± 0.8 days between periastron passage and flare center was also reported by WS, albeit with low significance. We confirm the small time difference of ~ 1.4 days but with improved significance.

Because the binary system GX 301-2/Wray 977 has an appreciable orbital eccentricity, the periodic outbursts in the X-ray light curve might be explained in the context of the eccentric-orbit accretion models discussed by Avni, Fabian, and Pringle (1976) and Okuda and Sakashita (1977). Although such models qualitatively reproduce the overall shape of the X-ray light curve (KRP; WWC; WS), the model does not account for the fact that the flares peak before periastron passage. Hence, some other mechanism, not included in this model, may be required to interpret the difference in phase between the flare peaks and periastron passage. WWC suggested the absorption effect caused by a trailing wake behind the neutron star to explain the difference. In fact, such an enhanced absorption was measured with the *HEAO 1* A-2 experiment at phase 0.05 (WS). It is interesting to note that the time of X-ray maxima occurs when the neutron star is approximately along the line of sight to the companion star (see Fig. 3). Further observations, particularly to obtain high-quality X-ray spectra around the time of flare center and periastron passage, will be required to reveal the mechanism responsible for the phase difference.

The present collaborative work became possible thanks to the coordination efforts of Professor M. Oda. F. N. is grateful to Professor S. Hayakawa for his continuous encouragement and valuable discussions. We express our thanks to Professor Y. Tanaka and the members of the *Tenma* team for the use of a portion of the results obtained from the GX 301-2 observation with *Tenma*.

REFERENCES

Avni, Y., Fabian, A. C., and Pringle, J. E. 1976, *M.N.R.A.S.*, **175**, 297.
Bord, D. J., Mook, D. E., Petro, L., and Hiltner, W. A. 1976, *Ap. J.*, **203**, 689.
Boynton, P. E., Deeter, J. E., Lamb, F. K., Zylstra, G., Pravdo, S. H., White, N. E., Wood, K. S., and Yentis, D. J. 1984, *Ap. J. (Letters)*, **283**, L53.
Bradt, H. V., *et al.* 1977, *Nature*, **269**, 21.
Hammerschlag-Hensberge, G., Zuiderwijk, E. J., van den Heuvel, E. P. J., and Hensberge, H. 1976, *Astr. Ap.*, **49**, 321.
Joss, P. C., and Rappaport, S. A. 1984, *Ann. Rev. Astr. Ap.*, **22**, 537.

Kawai, N., *et al.* 1985, *Pub. Astr. Soc. Japan*, **37**, 647.
Kelley, R., Rappaport, S., and Petre, R. 1980, *Ap. J.*, **238**, 699 (KRP).
Makino, F., Leahy, D. A., and Kawai, N. 1985, *Space Sci. Rev.*, **40**, 421.
Mauder, H., and Ammann, M. 1976, *IAU Circular*, No. 2980.
Mitani, K., Matsuoka, M., Makishima, K., and Inoue, H. 1984, *Ap. Space Sci.*, **103**, 345.
Nagase, F., *et al.* 1984, *Ap. J.*, **280**, 259.
Okuda, T., and Sakashita, S. 1977, *Ap. Space Sci.*, **47**, 385.
Pakull, M. 1978, *IAU Circular*, No. 3317.
Parkes, G. E., Mason, K. O., Murdin, P. G., and Culhane, J. L. 1980, *M.N.R.A.S.*, **191**, 547.
Priedhorsky, W. C., and Terrell, J. 1983, *Ap. J.*, **273**, 709.
Ricker, G. R., McClintock, J. E., Gerassimenko, M., and Lewin, W. H. G. 1973, *Ap. J.*, **184**, 237.
Rothschild, R., and Soong, Y. 1983, *Bull. AAS*, **15**, 940.
———. 1985, in preparation.
van Genderen, A. M. 1977, *Astr. Ap.*, **54**, 733.
Vidal, N. V. 1973, *Ap. J. (Letters)*, **186**, L81.
Watson, M. G., Warwick, R. S., and Corbet, R. H. D. 1982, *M.N.R.A.S.*, **109**, 915 (WWC).
White, N. E., Mason, K. O., Huckle, H. E., Charles, P. A., and Sanford, P. W. 1976, *Ap. J. (Letters)*, **209**, L119.
White, N. E., Mason, K. O., and Sanford, P. W. 1978, *M.N.R.A.S.*, **184**, 67p (WMS).
White, N. E., and Swank, J. H. 1984, *Ap. J.*, **287**, 856 (WS).

N. KAWAI: Institute of Space and Astronautical Science, 4-6-1 Komaba, Meguro-ku, Tokyo 153, Japan

R. L. KELLEY: Laboratory for High Energy Astrophysics, NASA/Goddard Space Flight Center, Greenbelt, Maryland 20771

F. NAGASE and N. SATO: Department of Astrophysics, Faculty of Science, Nagoya University, Furo-cho, Chikusa-ku, Nagoya 464, Japan

S. RAPPAPORT: Department of Physics and Center for Space Research, Massachusetts Institute of Technology, Cambridge, MA 02139

N. E. WHITE: ESA-Space Science Department, EXOSAT Observatory, ESOC, Robert Bosch Strasse 5, 610 Darmstadt, Federal Republic of Germany